Kovove Mater. 48 2010 257–263
DOI: 10.4149/km_2010_4_257

Studies on weldability of nichrome-laminated powder alloy using TIG welding

C. Z. Xia[1], Y. J. Li[1]*, J. Wang[1], U. A. Puchkov[2], Y. N. Jiang[1]

[1]*Key Laboratory for Liquid-Solid Structural Evolution and Processing of Materials (Ministry of Education), Shandong University, Jinan 250061, China*
[2]*Materials Science Department, Bauman Moscow State Technical University, Moscow, Russia*

Received 15 April 2010, received in revised form 21 April 2010, accepted 25 May 2010

Abstract

The objective of this study was to investigate the weldability of a new laminated material based on nichrome powder alloy using tungsten inert gas welding. Results revealed that nichrome-laminated powder alloy could be successfully joined by TIG welding. Two typical fusion zones were formed between different layers (Ni cover layer and nichrome base layer) and weld metal. Moreover, fusion zone of nichrome powder alloy was jagged due to the presented porosity. Between nichrome powder alloy and the filler metal, elements diffusion was obvious and a transition zone about 80–85 μm was formed. Microhardness near the fusion zone of nichrome base layer side (210–250 MPa) is higher than that near the fusion zone of Ni cover layer (190–210 MPa). Phase constitutions of the welded joint consisted mainly of γ-Fe, δ-ferrite and γ-Ni (Fe, Cr). Furthermore, co-existing microstructure of γ austenite and a small amount of δ ferrite was observed in the weld seam.

K e y w o r d s: powder alloy, tungsten inert gas welding, fusion zone, fine structure

1. Introduction

In the last decades, powder metallurgy components have been attractive in replacing wrought or cast materials due to their excellent performances such as the controllability of alloy content and density and low cost [1–3]. They are widely used in energy, powder and aerospace industries. For some special applications, it may be necessary to join powder metallurgy parts to one similar or dissimilar material as integrated components. Therefore, weldability of powder components must be very well established [4, 5].

The welding of powder metallurgy components is complex due to the presence of internal porosities. Study on the weldability of powder metallurgy components has followed closely to the development of powder metallurgy technology and achieved an important breakthrough in the last twenty years [1, 6–9]. The weldability of powder metallurgy materials is closely related to its relative density. Depending on the relative density of powder metallurgy components, a suitable welding process should be designed [6, 8]. An excellent joint of powder metallurgy components could be obtained by controlling welding parameters, selecting suitable filler alloy, and retaining a good penetration ratio [1, 3, 4, 10–12].

Three difficulties have been identified in the welding process of this nichrome-laminated powder alloy. First, low melting phases and columnar austenitic grains are easily formed, resulting in segregation of impurities, and hot cracking sensitivity. Second, segregated phases formed during the solidification of weld metal, reduce plasticity in the welding zone. Third, when heated by a welding arc, the cover layer of the laminated materials is easily separated from the base layer, inducing a weak connection [8, 13, 14]. It would be extremely significant to accelerate the application of this material if it was possible to achieve a satisfactory joint with excellent, crack-free characteristics.

Nichrome powder metallurgy was studied since the 1960s, and now the manufacturing technology has reached an advanced stage [15–17]. However, many works studying a weldability of high temperature powder metallurgy are related to iron based powder

*Corresponding author: tel.: +86-0531-88392924; fax: +86-0531-88392924; e-mail address: yajli@sdu.edu.cn

Table 1. Chemical compositions and mechanical properties of experimental materials

Materials	Mechanical properties		Chemical compositions (wt.%)							
	Tensile strength (MPa)	Elongation, δ_5 (%)	Ni	Cr	C	Mn	Si	Ti	S	P
18Cr-9Ni	520	40	8.0 ∼ 11.0	17.0 ∼ 19.0	≤ 0.12	≤ 2.00	≤ 1.00	0.5 ∼ 0.7	≤ 0.03	≤ 0.03
Cr25-Ni13 filler alloy	≥ 550	≥ 25	12.0 ∼14.0	22.0 ∼ 25.0	≤ 0.10	0.50 ∼ 2.5	≤ 0.90	Mo ≤ 0.75	–	Cu ≤ 0.75

Table 2. Welding technology parameters

Welding current (A)	Welding voltage (V)	Welding speed (cm s^{-1})	Argon flow (L min^{-1})
75–85	10–12	0.2	8–10

alloy. Research related to the weldability of nichrome powder alloy is sparse and no reports have been issued so far. Among all the joining methods mostly considered, tungsten inert gas welding (TIG) process can provide suitable results in many situations because of its flexibility in controlling parameters, such as heat input, travelling speed and type of filler alloy [1, 3, 4, 8, 10–12, 18, 19]. In this paper, TIG welding process was performed to study the weldability of a laminated material based on nichrome powder metallurgy. This nichrome-laminated powder alloy could be used in manufacturing components for aerospace, energy and chemical industries, which is necessary to withstand high temperature and corrosion [20].

2. Experimental details

Materials used were a sandwich plate comprised of a super Ni cover layer (Ni > 99.5 %) and a Ni80--Cr20 base layer (Fe < 0.6 %). Ni80-Cr20 base layer was a kind of nichrome based powder alloy. Relative density of Ni80-Cr20 base layer was 6.77 g cm^{-3} and porosity ratio was about 35.4 %, determined by digital image analysis techniques. The stainless steel was 18Cr-9Ni austenitic steel and the filler alloy was Cr25-Ni13 wire. Thickness of the nichrome-laminated powder alloy and 18Cr-9Ni stainless steel is 2.6 mm. The chemical composition and mechanical properties of the studied materials are given in Table 1.

The oxidation film and surface contamination of the materials were removed by mechanical and chemical methods before welding. A butt joint of the nichrome-laminated powder alloy and the austenite steel plate was designed and subsequently welded by tungsten inert gas welding (TIG) process with Cr25--Ni13 filler alloy. Main welding parameters are given in Table 2. Because the thickness of the welded materials is only 2.6 mm, a low welding current is necessary and the direction of welding arc should be controlled towards 18Cr-9Ni stainless steel side.

Detailed microstructures of weld interface were examined by optical microscope and scanning electronic microscopy (SEM). Samples were cut from the joints using electro-discharge machining, ground using different grades of sand paper, polished and finally etched with a mixed solution of HCl, HNO_3 and CH_3COOH (1 : 3 : 4) to examine the finer details of the microstructure. Microhardness was measured near the fusion zone of nichrome-laminated powder alloy side, via Shimadzu microsclerometer at a load of 50 gf.

A typical element distribution perpendicular to the interface of Ni80-Cr20 base layer and weld seam was measured via line scanning with X-ray dispersive spectrometer. Phase constitution was studied by means of X-ray diffraction (XRD).

Metallographic samples and thin slice samples were cut from the joint using electro-discharge machining, ground and polished. The slice samples were abraded into thickness 50 μm, and then prepared as thin film samples by electrolysing corrosion for transmission electron microscopy (TEM) and electron diffraction analysis (EDA).

3. Results and discussion

3.1. Macro photography and cross-section of the welded joint

In general, the metallurgy connection between different layers of the laminated material and the filler alloy is difficult. Specially, for a laminated material with a cover layer only 0.3 mm, molten loss phenomenon of the cover layer is prone to induce failure of the welding process. Typical macro photography of the welded

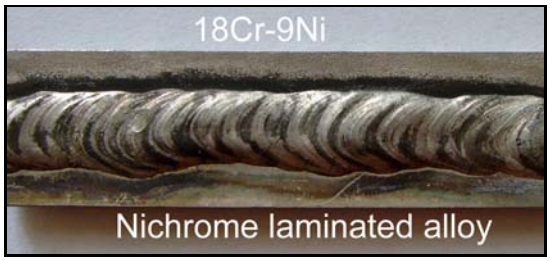

Fig. 1. Macrophotography of the welded sample.

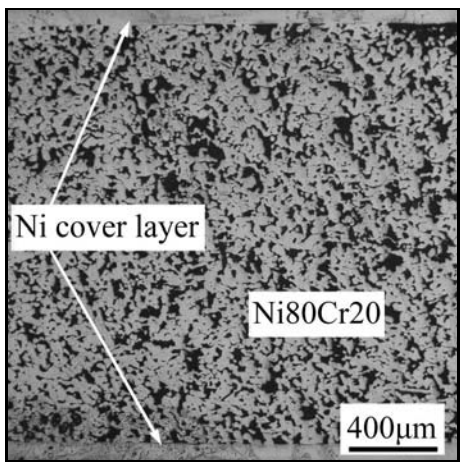

Fig. 2. Section of the nichrome-laminated powder alloy.

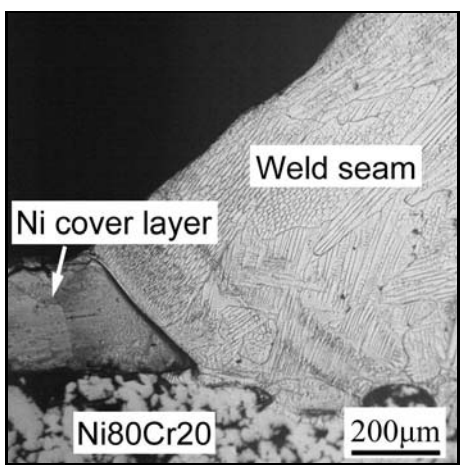

Fig. 3. Cross section of the weld near the nichrome--laminated alloy side.

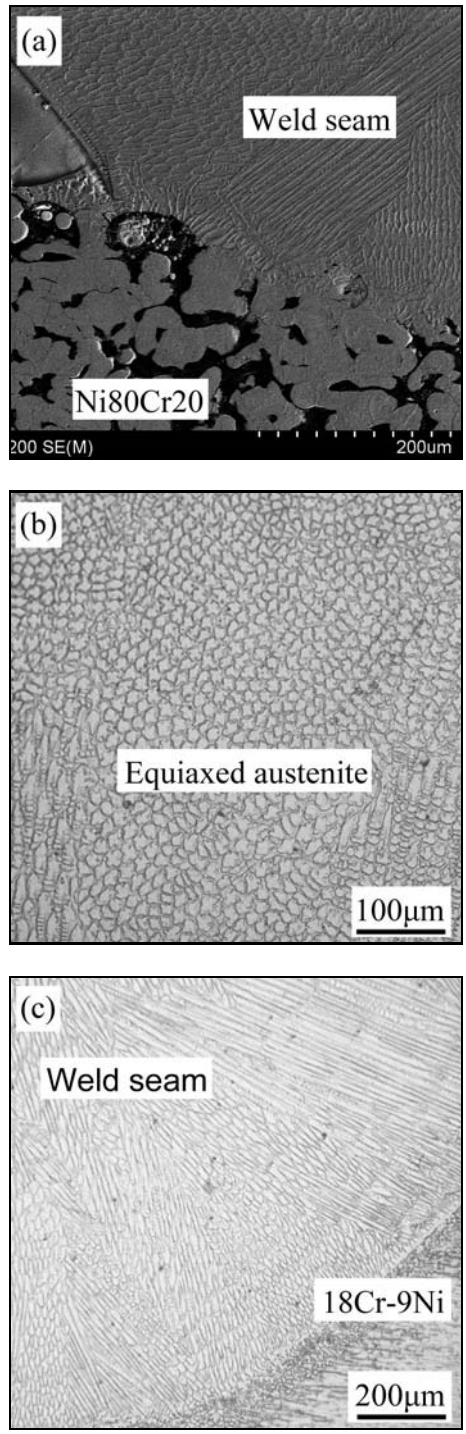

Fig. 4. Microstructure of the nichrome-laminated alloy joint: (a) fusion zone of the nichrome-laminated powder alloy side, (b) weld seam, (c) fusion zone of the 18Cr-9Ni steel side.

samples is presented in Fig. 1. Sound weld seam surface was formed.

3.2 Microstructure of the fusion zone

Section of the nichrome-laminated powder alloy is shown in Fig. 2. White bone-shaped base metal is of austenite structure with small cellular subgrains. Compact microstructure in the Ni-Cr base layer was formed after vacuum sintered and pressed. Valid metallurgy connection was formed between the nichrome--laminated powder alloy and the weld metal (see

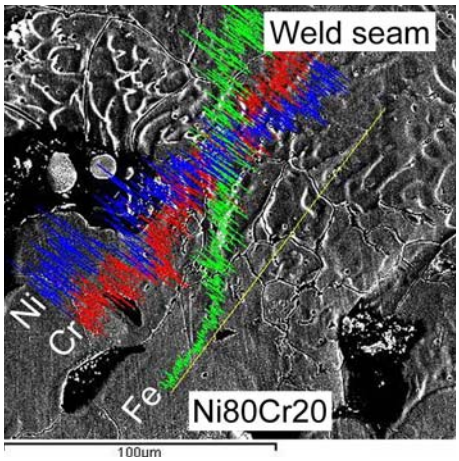

Fig. 5. Typical elements distribution near the fusion zone of nichrome alloy.

Fig. 3). Microstructure feature of the fusion zone and the weld seam of the laminated materials dissimilar joints are illustrated in Fig. 4. Two different regions were formed in the weld cross section: one is fusion zone between Ni cover layer and the weld metal and the other is fusion zone between Ni80Cr20 base layer and the weld metal (see Fig. 4a).

Different to traditional wrought or cast alloys, the fusion zone of nichrome powder alloy was jagged due to the presented porosity (see Fig. 4a), similar to the feature of iron based powder alloy welded [8].

Grain size in the fusion zone was smaller than that in Ni80Cr20 base layer. In the weld metal, the columnar crystals grew perpendicular to the fusion zone and large grain boundary was formed among different columnar crystal druses. The fusion zone between Ni cover layer and the filler alloy was narrow.

The main phase in the weld seam is equiaxed austenite grain with a partial remelting feature existing (see Fig. 4b). A sound metallurgical connection was formed between the 18Cr-9Ni steel and the weld seam (see Fig. 4c).

3.3. Element distribution between nichrome base layer and the weld

For further studying the typical elements transition between the nichrome alloy and the weld metal, the line scanning near the fusion zone of nichrome powder alloy was done by X-ray dispersive spectrometer and the results are presented in Fig. 5.

Elements diffused obviously from partial nichrome base metal melting. The transition zone has a width about 80–85 μm. Fe transited from the filler alloy to the nichrome powder base metal, while Ni was opposite, transited from the nichrome-laminated powder alloy to the weld metal. The transition of Cr was not obvious due to its content nearly equal in the base

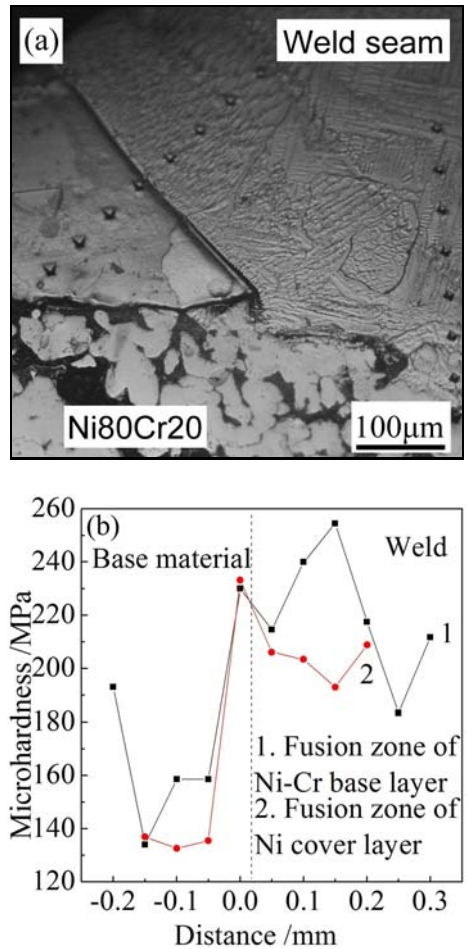

Fig. 6. Microhardness near fusion zone of nichrome-laminated powder alloy: (a) testing location, (b) microhardness profile.

metal and weld. Valid metallurgy joining was benefit from these elements transition between the filler alloy and base metal. The transition of Ni from the nichrome powder alloy to the weld mainly resulted in the formation of austenite phase.

While only 18Cr-9Ni steel was welded with filler wire Cr25-Ni13 alloy, some ferrite existed in the weld seam. However, in the condition of this paper discussed, lots of austenitizing Ni element from the nichrome-laminated alloy diluted into the weld inducing the content of Ni element increasing. Therefore content of ferrite was cut down heavily in the weld seam and only a small amount of ferrite formed and distributed on the austenite grain boundary. The ferrite pattern was difficult to be distinguished in the metallograph.

3.4. Microhardness near the fusion zone of nichrome alloy

Microhardness testing results are shown in Fig. 6.

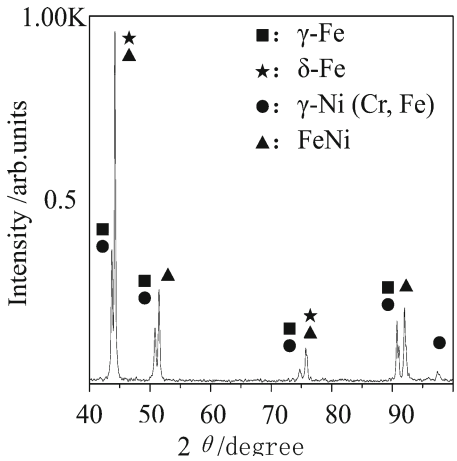

Fig. 7. X-ray diffraction patterns of welded joint of nichrome-laminated powder alloy and 18Cr-9Ni steel joint.

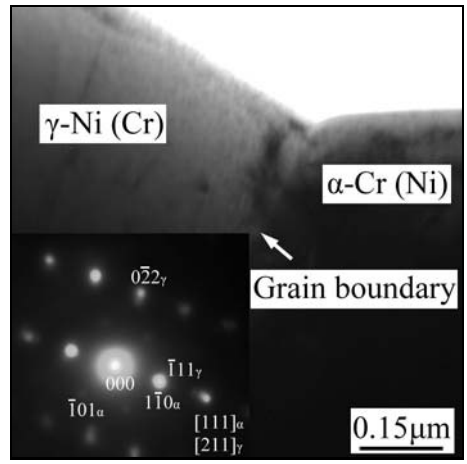

Fig. 8. TEM morphology and electron diffraction pattern of Ni-Cr powder alloy.

It can be found that microhardness in the weld is obviously higher than that in the nichrome-laminated alloy. Microhardness near the fusion zone of Ni80Cr20 base layer is 210–250 MPa, while that near the fusion zone of Ni cover layer is 190–210 MPa. This difference was concerned with the Cr concentration in various regions of the weld.

The concentration of Cr near the fusion zone of Ni80Cr20 base layer side was higher than that near the Ni cover layer due to the diluteness of pure Ni from Ni cover layer transited into the weld. The higher the concentration of Cr in the phases, the higher the microhardness value was. Microhardness of the Ni80Cr20 base layer was higher than that of Ni cover layer. Meanwhile the different cooling speed in various parts of the joint was also an important factor influencing microhardness.

3.5. XRD analysis near the fusion zone of the laminated composite side

To further clarify the phase constitution of the welded joint, XRD analysis method was adopted. XRD analysis was carried out under the following conditions: working voltage 60 kV and working current 40 mA. The results are shown in Fig. 7.

According to the XRD results, the welded joint consisted mainly of γ-Fe, δ-ferrite and γ-Ni (Fe, Cr) phase. Because of the transition of Ni element from the molten laminated composite, γ-Ni (Fe, Cr) phase was formed. And there are two kinds of austenite phase γ-Fe and γ-Ni (Fe, Cr) existing.

3.6. TEM analysis of base material and the welded joint

The fine structure and orientation relationship of grain lattice were studied for further discovering nature of the welded joint of the nichrome-laminated alloy. The micrograph of Ni-Cr powder alloy presented in Fig. 8 was obtained using a composite reflection of α [111] and γ [211]. The main phases of the Ni-Cr powder alloy are α-Cr (Ni) and γ-Ni (Cr) phase. Because of high resistance of electrolysing corrosion of Cr, area rich in Cr element of the sample was more difficult with electrolysing corrosion method than area rich in Ni element. So area rich in Cr emerged in high grey scale. The relationship between crystal plane $(1\bar{1}0)$ of α-Cr (Ni) and the crystal plane $(\bar{1}11)$ of γ-Ni (Cr) is parallel.

Different to the nichrome-laminated alloy, the main phases in the weld seam are γ-Fe austenite and δ ferrite. Part of Ni element transited from the molten laminated alloy participated in forming γ-Fe austenite, meanwhile some Ni involved in forming γ-Ni (Fe, Cr) austenite with Fe element in the weld seam. Under the non-equilibrium solidification condition in welding, as the rapid cooling speed, γ-Ni (Fe, Cr) phase still existed in the weld seam. The solution reaction was shown as follows:

$$\gamma\text{-Ni}\,(\text{Cr}) + \text{Fe} \rightarrow \gamma\text{-Ni}\,(\text{Fe}, \text{Cr}), \tag{1}$$

$$\text{Ni} + \gamma\text{-Fe} \rightarrow \gamma\text{-Fe}\,(\text{Ni}, \text{Cr}). \tag{2}$$

Typical micrograph of the weld seam is presented in Fig. 9. Analysed by means of selected area diffraction, a composite diffraction of γ [211] and δ-Fe [111] existed in this area. The relationship between the crystal plane $(\bar{1}11)$ of δ phase and the crystal plane $(1\bar{1}0)$ of γ phase is parallel. This result is a positive proof of the ferrite existing in the weld seam. If only austenite existed in the weld seam, solidification crack was easily to be formed in this region. Generally, a weld seam with austenite phase and about 5–10 percent of δ ferrite co-existing feature would be more expected [21].

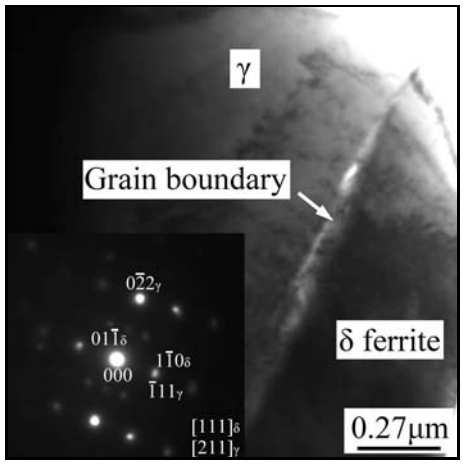

Fig. 9. TEM morphology and electron diffraction pattern of the weld seam.

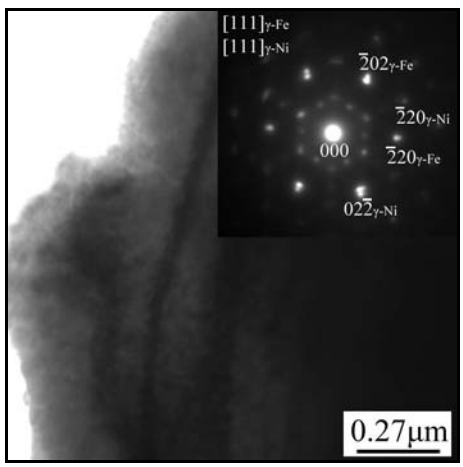

Fig. 10. TEM morphology and electron diffraction pattern of the fusion zone.

A small amount of ferrite existed in the weld seam played an important role in reducing internal stress and hot cracking tendency and improving the combination property of the welded joint.

In the fusion zone of the laminated alloy joint, a special composite diffraction of γ-Fe and γ-Ni (Fe, Cr) phase was observed (see Fig. 10) other than the existence of γ and δ phase. Due to the element dilution of the nichrome-laminated alloy and the rapid cooling speed, there are γ-Fe and γ-Ni (Fe, Cr) phases co-existing in the weld seam. So the inhomogeneity phenomenon of phases is obvious in the weld seam. This would promote the residual stress level, and made it difficult to control the overall performance of the welded joint.

4. Conclusion

1. Nichrome-laminated alloy may be successfully joined by tungsten inert gas welding. Two fusion zones were formed between both layers (Ni cover layer and nichrome base layer) and weld metal. The fusion zone between nichrome alloy and weld metal was jagged due to the present porosity.

2. There is a diffusion of Fe and Ni in the fusion zone. Fe diffused from the filler metal to the nichrome base metal and Ni diffused from the nichrome-laminated alloy to the weld metal. Width of the transition zone was about 80–85 μm. Microhardness near the fusion zone of Ni80Cr20 base layer is 210–250 MPa, higher than that near the fusion zone of Ni cover layer (190–210 MPa).

3. Phase constitutions of Ni-Cr powder alloy included α-Cr (Ni) and γ-Ni (Cr) phases and the welded joint consisted mainly of γ-Fe, δ-ferrite and γ-Ni (Fe, Cr) phase. There were two kinds of austenite, γ-Fe and γ-Ni (Fe, Cr) co-existing in the weld seam due to the transition of Ni, Cr element in the welding process. Meanwhile the co-existing microstructure of γ austenite and a little δ ferrite was observed in the weld seam and the lattice orientation between δ and γ phases was $(\bar{1}11)_\delta // (1\bar{1}0)_\gamma$.

Acknowledgements

This project was supported by the National Natural Science Foundation of China (grant no. 50874069) and the Research Fund for the Doctoral Program of Higher Education (grant no. 200804220020).

References

[1] KURT, A.—ATES, H.—DURGUTLU, A.—KARACIF, K.: Weld. J., *83*, 2004, p. 34.
[2] CORREA, E. O.—COSTA, S. C.—SANTOS, J. N.: J. Mater. Process. Tech., *198*, 2008, p. 323. doi:10.1016/j.jmatprotec.2007.07.007
[3] SURESH, M. V.—KRISHNA, B. V.—VENUGOPAL, P.—RAO, K. P.: Powder Metall., *47*, 2004, p. 358. doi:10.1179/003258904225020783
[4] CORREA, E. O.—COSTA, S. C.—SANTOS, J. N.: J. Mater. Process. Tech., *209*, 2009, p. 3937. doi:10.1016/j.jmatprotec.2008.09.008
[5] RAO, S. S.—JAYABHARATH, K.—ASHFAQ, M.—KRISHNA, B. V.: Sci. Technol. Weld. Join., *11*, 2006, p. 183.
[6] FILLABI, M. G.—SIMCHI, A.—KOKABI, A. H.: Mater. Design, *29*, 2008, p. 411.
[7] HAMILL, J. A.: Inter. J. Powder Metall., *27*, 1991, p. 363.
[8] HAMILL, J. A.: Met. Powder Metall., *62*, 2007, p. 22. doi:10.1016/S0026-0657(07)70106-6
[9] JAYABHARATH, K.—ASHFAQ, M.—VENUGOPAL, P.—ACHAR, D. R. G.: Mat. Sci. Eng. A, *454*, 2007, p. 114. doi:10.1016/j.msea.2006.11.026
[10] CORREA, E. O.—COSTA, S. C.—SANTOS, J. N.: CIT Informacion Tecnologica (Chile), *11*, 2000, p. 109.
[11] SURESH, M. V.—KRISHNA, B. V.—VENUGOPAL, P.—RAO, K. P.: T. Indian I. Metals. *56*, 2003, p. 375.

[12] SURESH, M. V.—KRISHNA, B. V.—VENUGOPAL, P.—RAO, K. P.: Sci. Technol. Weld. Join., 9, 2004, p. 362. doi:10.1179/136217104225012238
[13] LU, W.—NAKAO, Y.—SHINOZAKI, K.: Trans. China Weld. Inst., *14*, 1993, p. 186.
[14] ENGSTROEN, H.—DURAN, J.—AMO, J. M.—VAZQUEZ, A. J.: J. Mater. Sci., *31*, 1996, p. 5443. doi:10.1007/BF01159315
[15] BELITSKII, M. E.: Powder Metall. Met. Ceram., *4*, 1965, p. 741. doi:10.1007/BF00774223
[16] SOLONIN, S. M.—KATASHINSKII, V. P.: Powder Metall. Met. Ceram., *42*, 2003, p. 235. doi:10.1023/A:1025755225969
[17] KUZNETSOV, E. I.—SATANIN, V. A.: Strength Mater., *15*, 1983, p. 1756. doi:10.1007/BF01523163
[18] HAMILL, J. A.: Weld. J., *72*, 1993, p. 37.
[19] ASM Handbook Committee: ASM Handbook. Vol. 7. Powder Metal Technologies and Applications. Ohio, ASM International 1998.
[20] CHEN, Y. L.: Aviat. Mainten. Eng., *5*, 2001, p. 10.
[21] FOLKHARD, E.: Welding Metallurgy of Stainless Steel. Vienna, Springer-Verlag 1988.